

5. T. S. Laslo, R. E. Cannon, and P. I. Sheehan, "Emittance measurements of solids above 2000°C," *Solar Energy*, 8, No. 4, 105-111 (1964).
6. E. G. Kuzovkov, V. V. Pasichnyi, V. S. Dvernyakov, and V. N. Sergeev, "Influence of sealed pyrometric devices on the heating of specimens undergoing high-temperature testing," *Teplofiz. Vys. Temp.*, 10, No. 1, 153-156 (1972).
7. G. A. Frolov, V. S. Dvernyakov, and V. V. Pasichnyi, "Results of an experimental investigation of heat transfer at a surface with the combined actions of radiative-convective sources of heat," *Teplofiz. Vys. Temp.*, 16, No. 1, 221 (1978).
8. Yu. V. Polezhaev and F. B. Yurevich, *Heat Shield* [in Russian], Énergiya, Moscow (1976).

MODEL FOR THE CALCULATION OF THE COMPLEX HEAT TRANSFER
IN HIGH-TEMPERATURE IR EMITTERS

N. A. Prudnikov, A. P. Dostanko,
M. Kh.-M. Tkhostov, and Yu. M. Sotnikov-Yuzhik

UDC 536.3

A mathematical model of the complex heat transfer in high-temperature IR emitters is proposed, together with a procedure for its numerical realization.

Recently, the technique of infrared heating has been steadily more widely used in technological processes of the radioelectronics industry, precision engineering, and other branches of the national economy. In particular, the modules for IR heating first proposed by the present authors and produced on the basis of series halogen quartz lamps have proved effective for high-temperature processes [1].

However, in designing the corresponding equipment, considerable difficulties arise because of the inadequacies of existing methods of calculating the radiational and complex heat transfer, both in the IR module itself and in the working volume of the thermoradiational devices. The main problem of module design here is the determination of the temperature of its quartz shell, which must be in the range 700-1250°K. A lower temperature leads to disruption of the halogen cycle, and hence to a sharp reduction in the life of the lamp, while a higher temperature reduces the mechanical strength of the quartz shell, which may lead to its rapid breakdown. In addition, calculation of the heat transfer in the working volume requires a knowledge of the spectral composition of the IR-module radiation, which depends not only on the supplied potential but also on the structure of the module.

The most general version of the module structure will be considered (Fig. 1a). It consists of a tungsten spiral 1, enclosed in a gas-filled quartz shell 2, which, within the limits of the angle β , is coated externally with a highly reflective metallic layer. Between the frame 3 and the reflective coating, there circulates a cooling fluid. Energy transfer within the shell 2 occurs both by radiation and by convection.

The free surface of the shell is surrounded externally by air, and may be subjected to the influence of external radiation. In view of the symmetry of the problem, only the half-length of the cylindrical-shell cross section will be considered. Taking the relatively small thickness of shell 2 in comparison with its radius into account, its temperature field is calculated in a plane approximation (Fig. 1b). For the formulation of the mathematical model, the following additional conditions are assumed: 1) the temperature and heat-transfer coefficients from the shell to the gas on both sides are known and constant; 2) the quartz shell absorbs and emits energy, but does not scatter it; 3) the spiral and the shell are non-gray bodies, whose specific heat, thermal conductivity, and radiational properties do not depend on the temperature; 4) the radiation intensity of the spiral considerably exceeds the intensity of intrinsic emission of the shell and, in considering the energy transfer across the shell, the latter may be neglected.

A. V. Lykov Institute of Heat and Mass Transfer, Academy of Sciences of the Belorussian SSR, Minsk. Translated from *Inzhenerno-Fizicheskii Zhurnal*, Vol. 42, No. 5, pp. 798-805, May, 1982. Original article submitted March 26, 1981.

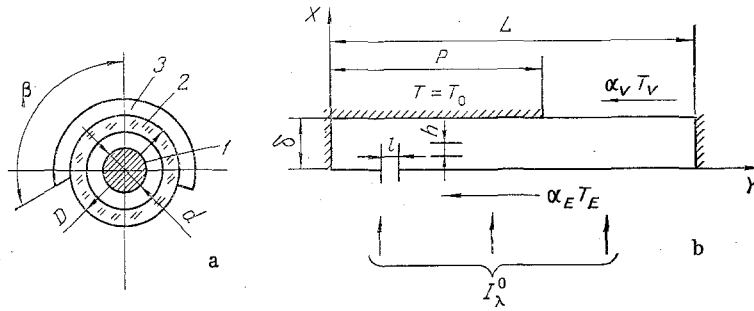


Fig. 1. Physical (a) and mathematical (b) calculation schemes for the emitter: 1) emitting tungsten spiral; 2) quartz shell; 3) cooling shell with reflective coating.

Under these conditions, the initial two-dimensional equation of heat conduction with internal sources may be split, according to the physical parameters, into two one-dimensional equations [2].

Taking account of the corresponding transfer equations, written by the Shuster-Schwartzschild method, the initial system of equations will take the following form: along the X axis

$$\frac{\partial \Theta'}{\partial Fo} = \frac{\partial^2 \Theta'}{\partial x^2} + \frac{\delta}{T_0 k} \int_{\gamma_2} Bu_\lambda (I_\lambda^R + J_\lambda^R) 2\varphi d\lambda, \quad (1)$$

$$I_\lambda^R(X) = [n^2 I_\lambda^0 (1 - R_1) + R_2 J_\lambda^C] \exp(-BuX), \quad (2)$$

$$J_\lambda^R(X) = [n^2 I_\lambda^0 (1 - R_1) + R_2 J_\lambda^C] R_2 \exp[-Bu] \exp[-Bu(1 - X)] \quad (3)$$

with the boundary conditions $\Theta'(X, Y, 0) = 1$, when $X = 0$:

$$-\frac{\partial \Theta'}{\partial X} = \frac{\delta}{kT_0} \int_{\gamma_2} [I_\lambda^0 \varphi - \pi B(\lambda, \Theta')] \varepsilon_\lambda d\lambda + Bi_e (\Theta_e - \Theta'), \quad (4)$$

$$I_\lambda = (1 - R_1) n^2 I_\lambda^0 + R_2 J_\lambda, \quad (5)$$

$$J_\lambda^e = (1 - R_2) \frac{J_\lambda}{n^2} + R_1 I_\lambda^e, \quad (6)$$

while

$$J_\lambda^C = \frac{I_e n^2 (1 - R_1) R_2 \exp(-2Bu)}{1 - R_2^2 \exp(-2Bu)}, \quad (7)$$

when $X = 1$, $Y \in L - p$:

$$\frac{\partial \Theta'}{\partial X} = \frac{\delta \pi}{kT_0} \int_{\gamma_2} \varepsilon_\lambda [J_\lambda^e - B(\lambda, \Theta')] d\lambda + Bi_a (\Theta_a - \Theta'), \quad (8)$$

$$J_\lambda = R_2 I_\lambda + (1 - R_2) n^2 J_\lambda^a, \quad (9)$$

$$I_\lambda^a = (1 - R_2) \frac{I_\lambda}{n^2} + R_1 J_\lambda^a, \quad (10)$$

when $X = 1$, $Y \in p$: $I = J$, $\Theta(1, Fo) = 1$; and along the Y axis

$$\frac{\partial \Theta}{\partial Fo} = \frac{\partial^2 \Theta}{\partial Y^2} + \frac{\delta}{T_0 k} \int_0^{\pi/2} \int_{\gamma_2} Bu_\lambda [I_\lambda + J_\lambda - 2n^2 B(\lambda, \Theta)] \sin \varphi d\varphi d\lambda, \quad (11)$$

$$\cos \varphi \frac{\partial I_\lambda}{\partial Y} = \alpha_\lambda (E_\lambda - I_\lambda), \quad (12)$$

$$\cos \varphi \frac{\partial J_\lambda}{\partial Y} = \alpha_\lambda (E_\lambda - J_\lambda) \quad (13)$$

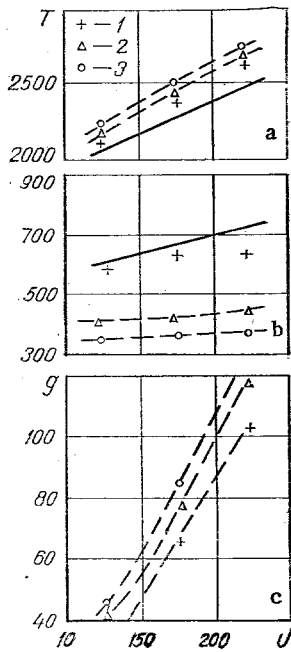


Fig. 2

Fig. 2. Dependence of the temperature of the spiral (a) and the quartz shell (b) and of the angular density of the radiation (c) on the applied potential: the continuous curves are the literature data [5, 6]; 1-3) calculation for $p = 0, 0.4, \text{ and } 0.6$, respectively. $T, ^\circ\text{K}$.

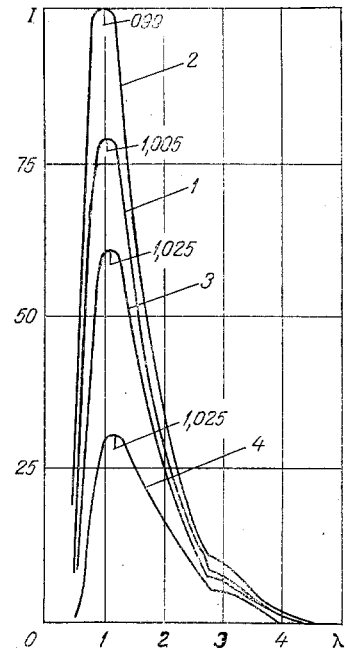


Fig. 3

Fig. 3. Dependence of the spectral composition of radiation from the module on the potential and its structure: $p = 0$ (1), 0.6 (2-4); $U = 220$ (1, 2), 175 (3), and 127 V (4). $\lambda, \mu\text{m}$; $I, \text{W/sr}\cdot\mu\text{m}$.

with the boundary conditions $\Theta_n(X, Y, F_0) = \Theta_{n-1}^i(X, Y, F_0)$ and

$$Y=0 \quad J=I, \quad \frac{\partial \Theta}{\partial Y} = 0; \quad Y=L \quad I=J, \quad \frac{\partial \Theta}{\partial Y} = 0. \quad (14)$$

Differential Eq. (1) describes the radiational-conductive heat transfer along the X axis, disregarding energy transfer in this direction due to the intrinsic emission of the quartz. Using Eqs. (2) and (3), the intensity of the radiation passing through the shell from the spiral may be calculated. Equation (7) is obtained from the limiting case of Eq. (2) and the boundary conditions in Eq. (5). In view of the intense cooling on the section 0-p, boundary conditions of the first kind are established there. Equation (11) describes the radiational-conductive heat transfer along the longitudinal axis Y, taking the intrinsic emission of the quartz in the semitransparent region γ_2 into account. The Fresnel formula is used to calculate R_1 and R_2 , which are the reflection coefficients at the air-glass and glass-air boundaries, respectively.

To determine the temperature of the spiral, the following balance equation is written

$$\frac{U^2 + \rho H}{\rho \eta \pi^2 L^c d} = \int_{\gamma_1 + \gamma_2 + \gamma_3} \epsilon_\lambda B(\lambda, T) d\lambda = AT^4, \quad (15)$$

where the first term defines the energy conducted to the spiral and the second the energy radiated there; $A \approx \epsilon \sigma_0 / \eta \pi \approx 0.7 \cdot 10^{-8} \text{ 1/deg}^4$, reduced emission coefficient, obtained after dividing all the parts of Eq. (15) by the dimensionless complex $\eta \pi$; $H = \pi^2 L^c d \int_{\gamma_1 + \gamma_2} J_\lambda^e d\lambda$, energy incident on the spiral after reflection from the mirrored coating of the shell; ρ , resistance of the spiral, Ω .

Then the spiral temperature may be determined iteratively from the discrepancy between the first two terms in Eq. (15). Introducing the notation

$$\left(\frac{U^2}{\rho \eta \pi^2 L^c d} + \frac{p}{\eta} \int_{\gamma_1 + \gamma_2} J_\lambda^e d\lambda \right) - \int_{\gamma_1 + \gamma_2 + \gamma_3} \epsilon_\lambda B(\lambda, T) d\lambda = \Sigma,$$

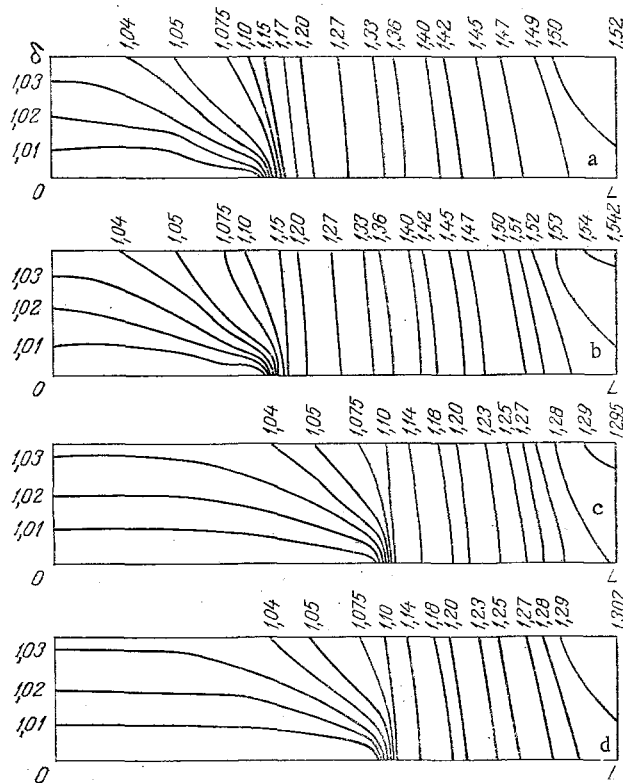


Fig. 4. Calculated temperature field of quartz shell, taking account of internal radiational transfer (a, c) and only of the heat-conduction mechanism (b, d) when $p = 0.4$ (a, b) and 0.6 (c, d) (the isotherms are given in dimensionless form, $\theta = T/T_0$, $T_0 = 290^\circ\text{K}$).

it follows that $\Sigma = A[(T_{i+1} + \Delta T)^4 - T_i^4]$, and hence, with acceptable accuracy and convergence, the following relation may be written

$$T_{i+1} = T_i + \frac{\Sigma}{3AT_i^3}. \quad (16)$$

The angle φ , within which the radiation from the spiral permeates the shell, may be simply determined from geometric considerations: $\varphi = 2d/\sqrt{D^2 - d^2}$.

The following procedure for solving the system in Eqs. (1)-(14) is possible. First, Eqs. (12) and (13) are transformed to give [3]

$$I_{i+1,\varphi} = I_{i,\varphi} \exp\left(\frac{-Bu l}{\cos \varphi}\right) + \bar{E} \left[1 - \exp\left(\frac{-Bu l}{\cos \varphi}\right)\right], \quad (17)$$

$$J_{i,\varphi} = J_{i+1,\varphi} \exp\left(\frac{-Bu l}{\cos \varphi}\right) + \bar{E} \left[1 - \exp\left(\frac{-Bu l}{\cos \varphi}\right)\right] \quad (18)$$

with the boundary conditions $I = J$; \bar{E} is determined from the mean temperature of the region, $\bar{\theta}_i = (\theta_i + \theta_{i+1})/2$. Equations (17) and (18) are solved by trial and error, to which end they are written in the form of recurrence relations

$$I_0 = c_0 J_0 + d_0, \quad (19)$$

$$I_{i+1} = a I_i + b_i, \quad (20)$$

$$J_i = a J_{i+1} + b_i, \quad (21)$$

where $c_0 = 1$; $d_0 = 0$; $c_N = 1$; $d_N = 0$; $a = \exp(-Bu l / \cos \varphi)$; $b_i = \bar{E}_i [1 - \exp(-Bu l / \cos \varphi)]$; $c_{i+1} = c_i a^2$; $d_{i+1} = b_i (1 + a l_i) + a d_i$; $J_N = R_2 d_N / (1 - R_2 c_N)$. Then the sequence of calculations in Eqs. (12) and (13) will be as follows. Determining c_i and d_i from the recurrence formulas, J_N is found. Finding J_i from Eq. (21), I_0 is calculated from Eq. (19), and then I_i from Eq. (20). The differential Eqs. (1) and (11) are written in grid form, and then solved by the trial and error method [4].

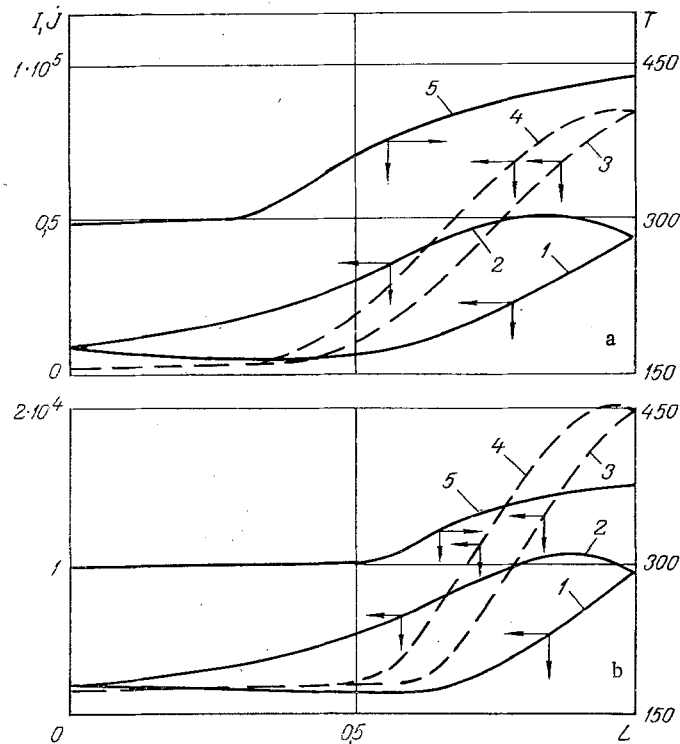


Fig. 5. The intensity variation of the intrinsic emission of the quartz shell I, J ($\text{W}/\text{m}^2 \cdot \text{sr} \cdot \mu\text{m}$) in the longitudinal direction at $p = 0.4$ (a) and 0.6 (b): 1, 2) I and J , respectively, at $\lambda = 3.75 \mu\text{m}$; 3, 4) I and J , respectively, at $\lambda = 4.00 \mu\text{m}$; 5) $f(L)$.

In the calculations, the spectral emissivity of the tungsten spiral calculated in [5] was used. The spectral emissivity and absorption coefficient of quartz were taken from [6]. The calculations were performed in the spectral interval $0.5\text{--}17 \mu\text{m}$ for a single lamp of type KG 220-1000.

The reliability of the results of numerical calculation was checked by comparing them with experimental data obtained in [7], for the case $p = 0$. The results of this comparison are shown in Fig. 2. The discrepancy between these data is no more than 8-9% for the shell temperature and 5-6% for the spiral temperature, which is completely acceptable for most engineering calculations.

The results of calculations for different degrees of screening show that the shell temperature for a single module in a free volume is sharply reduced, and is $350\text{--}450^\circ\text{K}$, while the spiral temperature due to self-irradiation rises by approximately $150\text{--}200^\circ\text{C}$. This leads to a significant increase in the intensity of emission of the spiral (Fig. 3) and the energy density emitted by the module in the given solid angle (Fig. 2c). The data shown in Fig. 2c are in good agreement with the results of [5, 7]. The discrepancy existing in the magnitude of the intensity is due solely to the difference in spiral temperatures taken as initial data. According to the data of the calculations, there is only an absorption band in the region of $2.75 \mu\text{m}$, which is not in [5, 7]. The spectral composition of the radiation depends strongly on the potential, but the position of the maximum is shifted extremely slightly here.

As follows from Fig. 3, the spectral radiation intensity of the module is determined by the radiation directly from the spiral even in the region $3\text{--}3.75 \mu\text{m}$. The semitransparency of quartz must be taken into account only in the vicinity of the strong absorption band at $2.75 \mu\text{m}$ and in the region $3.75\text{--}5 \mu\text{m}$. The intrinsic radiation of the shell in the region $5\text{--}17 \mu\text{m}$ may be disregarded for the cooled module, since the integral flux created by this radiation is less than 0.01% of the radiation from the spiral.

The dependence of the integral flux density in unit solid angle on the potential is given in Fig. 2c. Increase in the degree of screening leads to increase in flux density in the given direction by 25-30%, and reduction in the potential by 30% reduces the integral flux by half.

The form of the temperature field in the quartz shell under different conditions of cooling is demonstrated by means of isotherms in Fig. 4. As is evident from Fig. 4, the temperature gradient is directed radially in the cooling region, as in the case of a free shell. At the same time, when a portion of the shell is cooled, the gradient changes direction by 90° in its free part. The largest value of the gradient, as would be expected, is in the transitional region between the water-cooled section and the free section of the shell. When $p = 0.4$, the gradient in this region is $45^\circ\text{C}/\text{mm}$, while at $p = 0.6$ it reaches $55^\circ\text{C}/\text{mm}$. The character of the temperature field is determined mainly by the mechanism of heat conduction. Comparison of the temperature fields of the shell calculated both with the simultaneous action of radiational and conductive transfer (Fig. 4a, c) and with only conductive transfer (Fig. 4b, d) shows that at $p = 0.6$ no significant changes in the temperature field occur. At the same time, at $p = 0.4$, disregarding the radiational component leads to marked increase in shell temperature in the free region and to increase in the temperature gradients there.

The intensity of the intrinsic emission of the quartz over the perimeter of the shell is shown in Fig. 5. Heat transfer by radiation may only occur in the region where I and J have different values at the same point, i.e., where the "hysteresis loop" is broad. Analysis shows that the determining contribution to the radiational transfer occurs close to the $3.75\text{-}\mu\text{m}$ band. But, at ordinary shell temperatures, there is a maximum of the radiation close to this region, which also leads to a pronounced contribution of the radiational component to the total heat transfer.

Comparison of the contribution of the different mechanisms of heat transfer from the spiral to the internal surface of the shell shows that the convective energy supply from the heated gas is determining here. The contribution of direct radiation from the spiral in the given spectral region ($5\text{-}17\ \mu\text{m}$) is no more than 15-20%.

From a comparison of the results of the calculations (Figs. 3 and 4), it follows that the use of screened, water-cooled modules in high-temperature equipment allows the useful integral flux density from the radiator to be significantly increased, without causing heating of the quartz shell at the same time. From the data shown in Fig. 2, it follows that the use of such modules for low-temperature equipment is inexpedient, since the effective cooling leads to strong chilling of the shell, and this disrupts the regenerating halogen cycle, which is only operative at $t > 500^\circ\text{C}$.

The results of calculating the internal-radiation intensity in the shell (Fig. 5) confirms that this factor significantly influences the shell temperature and neglecting it may lead to serious errors.

NOTATION

λ , wavelength; k , thermal conductivity; I, J , spectral intensity of the radiation; α , absorption coefficient; n , refractive index; $E = n^2 B(\lambda, T)$, spectral intensity in the glass; $B(\lambda, T)$, Planck function; ϵ , emissivity; $\sigma_0 = 5.67 \cdot 10^{-8}$, Boltzmann constant; R_1, R_2, R_0 , reflection coefficients; $Bu = \alpha\delta$, Bouguer number; $Bi = \alpha\delta/k$, Biot number; $Sk = \sigma L T_0^3/k$, Stark number; $Fo = \alpha\tau/\delta^2$, Fourier number; $\theta = T/T_0$, dimensionless temperature; $\gamma_1 = 0.5\text{-}2\ \mu\text{m}$, spectral region of transparency of quartz; $\gamma_2 = 5\text{-}17\ \mu\text{m}$, region of nontransparency of quartz; $\gamma_3 = 2\text{-}5\ \mu\text{m}$, region of semitransparency of quartz; U , electrical potential; ρ , resistance; Ω ; d , conventional diameter of spiral winding; D , internal diameter of radiator shell; L^C , length of spiral; η , proportion of energy radiated from the spiral, radiant efficiency of spiral. Subscripts: e , values within shell; α , outside shell.

LITERATURE CITED

1. A. P. Dostanko, M. Kh.-M. Tkhostov, et al., Inventor's Certificate 760490, "Infrared-heating apparatus," Byull. Izobret., No. 32 (1980).
2. S. N. Godunov and V. S. Ryaben'kii, Difference Schemes [in Russian], Nauka, Moscow (1973).
3. A. A. Fauél et al., "Calculation program for determining the heat transfer through glass," Raketn. Tekh. Kosmon., 114-121 (1969).
4. N. S. Berezin and N. P. Zhidkov, Methods of Computation [in Russian], Vol. 2, Fizmatgiz, Moscow (1959).
5. D. V. Zvorykin and Yu. I. Prokhorov, Application of Radiant Infrared Heating in the Electronics Industry [in Russian], Energiya, Moscow (1960).

6. A. E. Sheindlin (ed.), Radiative Properties of Solid Materials (Handbook) [in Russian], Energiya, Moscow (1974).
7. Yu. I. Prokhorov and V. I. Ivanov, "Emission spectra of infrared incandescent tubes," Elektrotermiya, No. 112-113, 24-26 (1971).

NUMERICAL STUDY OF SPECTRAL INTENSITY OF EMISSION AND
ABSORPTION OF THE CO₂ AND CO MOLECULES UNDER
VIBRATIONALLY NONEQUILIBRIUM CONDITIONS

N. N. Kudryavtsev and S. S. Novikov

UDC 631.375

Numerical calculations are performed of the spectral intensity of emission and absorption of the 4.3- and 2.7- μm bands of CO₂ and of the 4.7- μm band of CO under conditions of nonequilibrium excitation of the vibrational degrees of freedom.

The development of spectroscopic methods of studying vibrationally nonequilibrium molecular media requires a detailed study of transport processes of IR radiation in the absence of equilibrium between vibrational and translational-rotational degrees of freedom. In the present paper we provide a numerical study of the effect of the parameters of a vibrationally nonequilibrium gas on the spectral intensity of emission and absorption of CO₂ in the 4.3- and 2.7- μm bands of CO₂ and the 4.7- μm band of CO. Several results of studying the effect of parameters of a vibrationally nonequilibrium gas on the integral characteristics of emission and absorption of these bands are presented in [1].

The calculation of spectral characteristics of emission and absorption was performed in a wide region of variation of the dominating parameters: pressure, translational and vibrational temperatures, including the conditions in regions of CO₂-laser resonator, vibrationally nonequilibrium supersonic flows containing CO₂ and CO, etc. The populations of the lowest 5-10 levels of each mode, the transitions between which basically determine radiation transport of a vibrationally nonequilibrium gas under the conditions considered, can be described by a Boltzmann distribution with a corresponding vibrational temperature [2].

The distribution of CO₂ molecules over vibrational levels was described by two temperatures. The vibrational temperature T_3 characterizes the distribution of molecules within an asymmetric mode, where T_2 is the collective (symmetric and deformational) mode. The possibility of introducing a single temperature for the symmetric and deformational types of vibration is related to the strong interaction of these modes due to Fermi resonance. The vibrational distribution of CO molecules was characterized by the temperature T_5 . The temperature of the rotational degrees of freedom of the CO and CO₂ was assumed equal to the translational one [2]. In the present paper we use the enumeration system of physical quantities for CO₂-lasers according to which the subscripts 2, 3 refer, respectively, to combined and asymmetric modes of CO₂, and 4 and 5 - to nitrogen and carbon monoxide [2].

The dependence of the emission intensity I_ω on the wave number at gas pressure $P = 10^{-3}$ - 10^{-1} atm, characteristic for a number of vibrationally nonequilibrium systems, changes strongly within narrow spectral regions, corresponding to a width of separate rotational lines and consisting of 10^{-2} - 10^{-4} cm^{-1} . The use of methods of the theory of vibrational-rotational bands [3] makes it possible to determine values of spectral intensities of emission I_ω and absorption A_ω averaged over the rotational structure. The averaging range is chosen to be $\Delta\omega' = 2$ - 10 cm^{-1} , corresponding to a nonsignificant variation of the values I_ω and A_ω , not exceeding 5-10% [3].

For the pressure values considered $P \leq 0.1$ atm the width of rotational lines γ in CO₂ and CO bands is smaller by 1-3 orders of magnitude than the separation between neighboring lines d [4]. Under these conditions the use of an isolated line model for calculating